Photo-activated Low Temperature, Micro Fuel Cell Power Source

FINAL SCIENTIFIC/TECHNICAL REPORT

Reporting period start date: 09/20/2005

Reporting period end date: 09/30/2007

Principle author: Harry L. Tuller

Date Report issued: January 2008

DOE Award number: DE-FC26-05NT42624

Name and address of submitting organization:
Massachusetts Institute of Technology
77 Massachusetts Avenue
Building E19-750
Cambridge, MA. 02139

ABSTRACT - A Key objective of this program is to identify electrodes that will make it possible to significantly reduce the operating temperature of micro-SOFC and thin film-based SOFCs. Towards this end, efforts are directed towards a) identifying the key rate limiting steps which limit presently utilized electrodes from performing at reduced temperatures, as well as, b) investigating the use of optical, as opposed to thermal energy, as a means for photocatalyzing electrode reactions and enabling reduced operating temperatures. During Phase I, the following objectives were achieved: a) assembly and testing of our unique Microprobe Thin Film Characterization System; b) fabrication of the model cathode materials system in thin film form by both PLD and ink jet printing; and c) the successful configuration and testing of the model materials as cathodes in electrochemical cells. A further key objective d) to test the potential of illumination in enhancing electrode performance was also achieved.

TABLE OF CONTENTS

I. EXECUTIVE SUMMARY

The electrochemical performance of electrodes is presently the key limiting factor in achieving satisfactory performance in micro-SOFC and conventional SOFC designed to operate at intermediate or reduced temperatures. Determining the rate limiting step/s remains a challenge from both scientific and technological standpoints, and despite extensive research efforts, no consensus exists about the rate limiting step/s in SOFC electrodes.

This program has several inter-related objectives. Most broadly, to identify electrodes that will make it possible to significantly reduce the operating temperature of micro-SOFC and thin film-based SOFCs. Towards that objective, key goals of this program include: 1) identify the key rate limiting steps limiting presently utilized electrodes from performing at reduced temperatures and 2) investigate the use of optical, as opposed to thermal energy, as a means for photocatalyzing electrode reactions and enabling reduced operating temperatures. This requires a multifaceted approach which addresses the need to a) work with well defined and reproducible electrode structures and model electrode compositions thereby enabling conclusions to be made about the rate limiting mechanisms controlling electrode performance that can then be broadly applied, b) utilize measurement techniques, including illumination, Kelvin Probe and Impedance Spectroscopy, which provide the ability to isolate the contributions of e.g. gas adsorption, charge transfer and diffusive kinetics towards the overall electrode impedance and c) offer prototype structures demonstrating reduced temperature operation and the potential advantages of illumination. This report summarizes progress achieved during the Phase I program.

In Phase I (one year's funding), we have focused on a) assembling and testing our unique Microprobe Thin Film Characterization System, b) demonstrating that the model materials system can be fabricated in thin film form, c) that it exhibits expected physical properties and d) that it can be configured and operated as model cathode material. A key objective was also to test the potential of illumination in enhancing electrode performance. These were all achieved as summarized below.

$SrTi_{1-x}Fe_xO_3$ (STF) was chosen as a model system given the ability to manipulate the band structure as well as the level of mixed ionic-electronic conduction by controlling the fraction of Fe substitution for Ti. We demonstrated that they could be *prepared systematically in thin film form* as a function of composition and that these films largely replicated the bulk materials properties whose defect, MIEC and optical properties were characterized and modeled in detail in earlier studies. Specifically a subset of STF films (x=0.05, 0.35 and 0.50) were prepared by PLD and ink jet printing and their properties were confirmed to exhibit expected characteristics.

Microelectrodes with varying diameters were fabricated and scaling with area was confirmed consistent with their mixed ionic-electronic conducting properties. Further they where shown to *exhibit typical electrode characteristics* when applied to solid electrolytes. A number of STF/YSZ/Pt and STF/YSZ/STF cells were prepared and studied by complex impedance spectroscopy over wide temperature limits (400-900C) and as a function of pO_2 ($pO2 = 1.5x10^{-2}$ to 1atm). The electrode impedance typically exhibited 3 impedance signatures, i.e. two somewhat overlapping semicircles at higher frequency and a 45° Warburg like contribution at reduced frequency and temperature. Of particular note, has been the demonstration of as much as a factor of 73% reduction in electrode impedance of $SrTi_{1-x}Fe_xO_3$ (x = 0.35) model electrode under low intensity illumination confirming the ability to modulate electrode impedance by illumination of a model electrode-electrolyte interface. In other cases, the effect of illumination was smaller.

Various techniques are used to examine surface or near surface properties of SOFC electrodes but are either limited to RT and high vacuum conditions (XPS, AES and SIMS) or are poor in their ability to monitor rapid kinetics (Impedance spectroscopy). We introduce the *Kelvin Probe (KP)*, which is non-invasive, yet is extremely sensitive to changes in the top-most atomic layer by measurement of the work function *WF*. The instrument installed in our microprobe system is based on the McAllister KP-6500 Kelvin probe, but the design was modified by us in collaboration with McAllister personnel to allow for a) high-temperature measurements (up to ca. 800°C) by incorporating water-cooling around the temperature-sensitive oscillation apparatus, and b) for surface photo voltage spectroscopy (SPS) measurements by incorporating a light-guide. Studies were initiated on LSC30 and STF35 while exposed to elevated temperature, controlled atmosphere and under illumination. The measurements, in response to changes in pO_2, were large, rapid and reversible with ability to resolve changes on the order of 10 mV. Increasing temperature was found to lead to decreasing *WF* consistent with expectation for increasing oxygen desorption. Transient *KP* measurements were consistent with the superposition of both chemisorption and bulk electrode effects. We also demonstrated the ability to operate under broad band illumination while performing the *KP* measurements under controlled temperature and pO_2.

In summary, during phase I, we focused on a) assembling and testing our unique Microprobe Thin Film Characterization System, b) demonstrating that the model materials system can be fabricated in thin film form, c) that they exhibit expected physical properties and d) that they can be configured and operated as model cathode materials. A key objective was also to test the potential of illumination in enhancing electrode performance. These were all achieved.

II. REPORT DETAILS

1. Experimental methods:

Electrochemical Impedance Spectroscopy (EIS) was performed with a Solartron 1260 instrument. The EIS measurements spanned a frequency range of 1 MHz to 1 mHz and a temperature range of 400°C to 900°C. An AC amplitude of 50mV was used throughout, as previous measurements had shown that this voltage lies within the linear regime of the sample's current-voltage response. A 100mV cathodic and anodic DC bias was applied to alter the electrochemical potential of oxygen at the electrode. Equivalent circuit representations consisting of resistors and constant phase elements (CPE) were employed to model and interpret experimental impedance data.

A Kelvin probe (McAllister Technical systems, KP6500) was utilized for in-situ work function measurements under controlled temperatures and gas compositions. The Kelvin Probe consists of a vibrating reference electrode in plane-parallel orientation to the sample, creating a capacitor. The sample and probe were connected via a voltage source known as the "backing potential" (V_b). When V_b is set to zero, a contact potential difference (V_{cpd}) equal to the difference in the probe and sample work functions is generated across the probe/sample faces. The change in work function is detectable because V_{cpd} is equivalent to the difference in work functions between the sample and reference. At the unique point where V_b=-V_{cpd}, the circuit is balanced and the electric field between the plates vanishes resulting in no output signal. This null condition and deviations from it can be detected with high precision, thereby directly measuring the changing sample work function. The Kelvin Probe System uses a digital oscillator and digital trigger which allows data to be recorded at a variety of frequencies and amplitudes. The reference plate of the probe was positioned approximately 0.5mm from the sample and operated at an oscillation frequency of 165 Hz. The backing potential was stepped in increments

of 500meV over a range of 2V and eight measurements were averaged for each applied potential. Labview programs were written to enable control of all equipment, including the stage temperature and gas flow rates, thus allowing for completely automated measurements. These programs are now accessible to our group via the internet for remote control and real-time visualization of measurements.

A unique microprobe system equipped with gas and temperature controls has been designed and constructed for both EIS and work function measurements. The system is comprised of a stainless steel vacuum chamber with a temperature controlled stage (HeatWave Labs, Watsonville, CA) capable of reaching up to 1,200^{o}C in air or other gas atmosphere. The chamber (built by McAllister Technical systems, Coeur d'Alene, ID) is equipped with four micro-manipulators that allow contact to micro-patterned electrodes with a spatial resolution of approximately 1 μm. The chamber consists of water-cooled double walls and a thermally isolated view port to prevent overheating. A stereo-microscope (Nikon SMZ1500) with coaxial illumination is used to provide high magnifications (up to 170x) at a large working distance (136mm) in order to position the probe tips on the micro-patterned electrode structures. The chamber is linked to a gas flow system (MKS 647C Mass Flow Programmer with four MKS 1359C Mass Flow Controllers and an MKS 628B Baratron Capacitance Manometer for pressure control) to control the gas composition inside the chamber. A turbomolecular vacuum system (Model TP-70-2DR, Janis Research Company, Wilmington, MA) enables measurements under vacuum conditions (~10^{-7} mbar), adjusts the total gas pressure, and refreshes the chamber from residual gases. The microprobe system includes thermocouples, pressure gauges, and an oxygen sensor to monitor the temperature, gas pressure, and oxygen partial pressure, respectively, during measurements.

A unique aspect of the microprobe system is the incorporation of a high-temperature Kelvin probe apparatus. This instrument is largely based on the McAllister KP-6500 Kelvin probe, but the design was modified by our group in collaboration with McAllister personnel to allow for a) high-temperature measurements (up to ca. 800°C) by incorporating water-cooling around the temperature-sensitive oscillation apparatus, adapted it to our microprobe system, and b) for surface photovoltage spectroscopy (SPS) measurements by incorporating a light-guide. A schematic drawing of the high-temperature Kelvin probe mounted on our microprobe system is shown in Fig. 1. Initial calibration of the Kelvin Probe was performed on Pt, STF and LSC electrodes. Because the Kelvin Probe is a very sensitive measurement tool, controlling noise levels is very important for its application. The predominant sources of error are stray capacitance and noise pickup. Stray capacitance is the largest source of errors in the Kelvin Probe caused by wires vibrating near charged insulators, or grounded conductors, inducing false signals in the preamp circuit. This effect is reduced by careful tuning of the Kelvin probe following the manufacturer's instructions. By calibrating the Kelvin Probe, we were able to obtain WF data with resolution within several mV even at elevated temperatures. The improvement in resolution is shown in Fig. 2

Two different thin film deposition techniques are used for this work. Pulsed Laser Deposition (PLD) is the commonly used especially for multi-component material systems because this technique gives good stoichiometric control. Ink-jet printing is another deposition technique for this study. The most important benefit of this method is ease and simplicity of sample preparation. As long as there are proper precursor solutions, any materials can be deposited by Ink-jet printing. Also, this is direct printing technique, so complex electrode patterning process, i.e. photoresist lithography, can be omitted. Therefore, ink-jet printing is potentially very useful as a secondary sample preparation tool. XRD, SEM, EDX, and AFM were used to characterize film composition and microstructures.

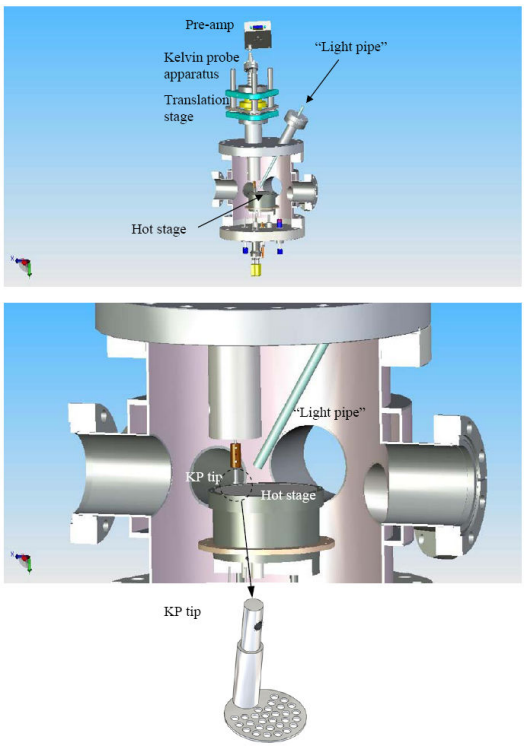

Figure 1: Schematic drawing of the high-temperature Kelvin probe apparatus.

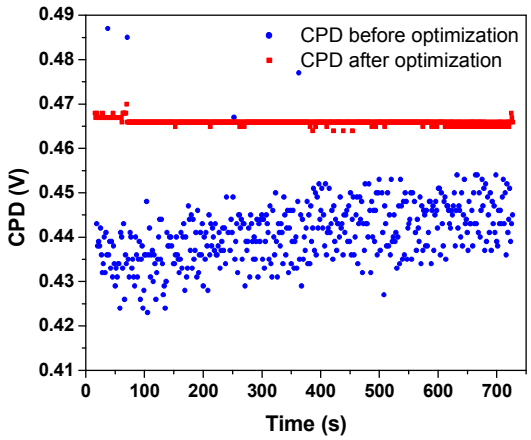

Figure 2: Kelvin Probe measurements of the Contact Potential Difference (CPD) of a Pt thin film on Si substrate at room temperature.

2. Results and discussions:

Many research efforts are being directed towards finding solutions that would enable operation at reduced temperatures (< 600°C) by adding special catalysts, by investigating new or modified materials and by attempting to enhance the reaction zone at the three phase boundaries between electrode, electrolyte, and gas phase. While these efforts are showing some success, progress is spotty and often not reproducible between different groups. We take a multifaceted approach which addresses the need to a) work with well defined and reproducible electrode

structures and model electrode compositions thereby enabling conclusions to be made about the rate limiting mechanisms controlling electrode performance, b) utilize measurement techniques, including illumination, Kelvin Probe and Impedance Spectroscopy, which provide the ability to isolate the contributions of e.g. gas adsorption, charge transfer and diffusive kinetics towards the overall electrode impedance and c) offer prototype structures demonstrating reduced temperature operation and the potential advantages of illumination. In the following, we review the approach being taken and the progress achieved during the one year funded Phase I program.

A. Well defined and reproducible electrode structures.

Lithographically defined thin film electrodes provide the opportunity to:

- systematically control and vary the triple phase boundary length (TPBL) and effective area of the electrodes.
- precisely control film thickness, grain size and orientation e.g. by controlled pulsed laser deposition or sputtering.
- prepare, *under clean conditions*, uncontaminated electrode-electrolyte interface.

Fig. 3 shows an example of LSC interdigitated electrodes on CGO Electrolyte fabricated in our laboratories[1]. Similar structures enabled us to precisely calibrate, for example, the electrode conductance of Pt on YSZ normalized to the triple phase boundary length (TPBL). Indeed, the electrode conductance scaled with TPBL[2]. For composite mixed conducting Pt/YSZ cermets, the conductance scaled instead with electrode area[3]. Thus, geometrically well defined electrodes enable one to identify, with confidence, where the active regions of the electrode are[4]. A very dramatic finding by our group for the Pt/YSZ system was that the electrode impedance could be increased *~1,000 fold* by careful control of the chemistry of the zirconia

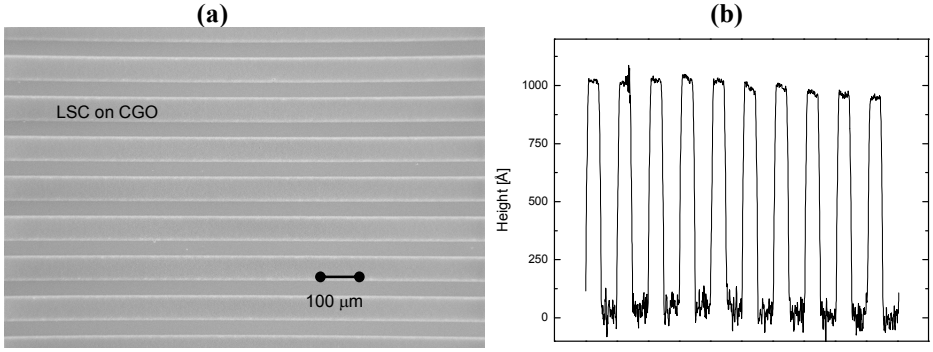

Figure 3: a) SEM image and b) surface profile of ~100nm thick microstructured LSC thin film electrode on thin film CGO (LSCO stripe = 50 μm, CGO stripe = 50 μm)[1].

surface[2]. By insuring a SiO_2 free surface, via reduced temperature vapor phase processing, the kinetics at the Pt/YSZ/air TPB could be enhanced by many orders of magnitude[2]. This is reflected in the recently reported low temperature operation of a similarly configured micro-fuel cell[5]. *We expect that improvements in performance of MIEC electrodes may be achieved by taking similar pains to insure clean electrode/electrolyte and electrode/gas interfaces.* Given our abilities to control surface chemistry by use of thin film process technology, this remains a focus of study.

In Phase I of this work, a number of model electrode structures were prepared including interdigitated electrodes and spherical microelectrodes with varying diameter. Examples are shown in Fig. 4. In this case, thin films of our model electrodes based on $SrTi_{1-x}Fe_xO_3$ (STF), *described in the next section*, were prepared for electrical characterization.

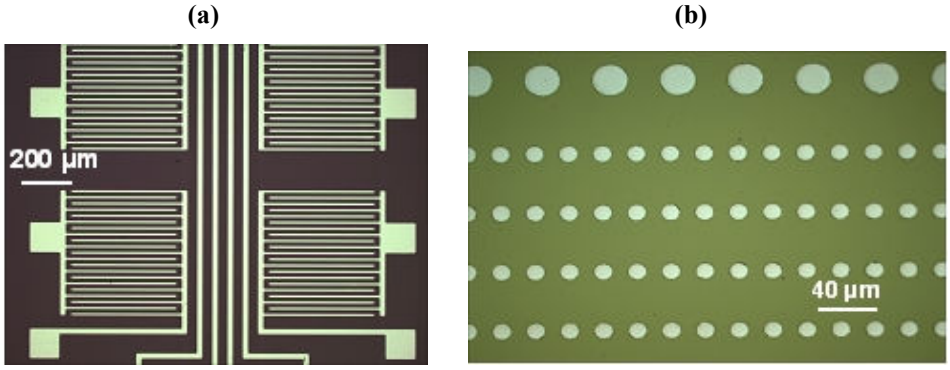

Figure 4: STF35 (x=0.35) films on MgO substrates with Pt electrodes sputtered onto the surface of the films in (a) interdigitated electrodes configuration, and (b) microcontact electrode configuration.

Subsequently, lithographically defined electrodes were prepared on YSZ to study their electrode behavior and help identify the active electrode sites, i.e. TPB or electrode area. Two types of structures were prepared. First, asymmetric structures in which STF electrodes were prepared on one side of the YSZ while the counter electrode was a large Pt electrode on the opposite side of the YSZ. Symmetric structures in which identical STF electrodes were deposited on both sides of the YSZ were also prepared. Electrical characterization of such structures is discussed below.

B. Model Electrode Materials

Mixed Ionic and Electronic Conductors (MIEC) such as $La_{1-x}Sr_xCoO_3$ (LSC) or $La_{1-x}Sr_xCo_{1-y}Fe_yO_3$ (LSCF) generally exhibit superior electrode performance in SOFCs. Yet, the details of why certain values of x and y in LSC and LSCF perform better are not understood. Thus, model electrode compositions, in which key parameters such as the magnitudes and ratios of the electronic and ionic conductivity (MIEC) and the corresponding energy states and bands can be systematically controlled, were selected. This offers the opportunity to vary these key parameters systematically and explore how the electrode impedance, photoresponse (see below) and work function respond in turn. We selected $SrTiO_3$ and its derivatives (e.g., $SrTi_{1-x}Fe_xO_{3-\delta}$) as the model system for our studies, given its well studied electronic structure,[6] optical properties,[7,8] defect chemistry,[9,10,11,12] electronic and ionic transport properties,[13,14,15,16] surface and grain boundary properties.[17,18,19,20] Our group has extensive experience with $SrTiO_3$ as a photoelectrode,[21] with its high temperature electrical properties, its defect structure and transport characteristics and its optical properties.[8,10,13] We have successfully grown high quality thin films of both $BaTiO_3$ and $SrTiO_3$ by pulsed laser deposition (PLD) and we can, by control of growth conditions, obtain textured films with desired crystallographic orientations and grain size.

$SrTiO_3$ can be easily doped on both A and B sites to tune its ionic and electronic conductivities. For instance, substituting Fe or Co for Ti leads to high mixed ionic-electronic conductivity, with total conductivities reaching ~10-100 S/cm (at T > 700°C in air) for high substitution levels.[22] While the predominant free carriers in these solid solutions are electrons at low oxygen pressures or holes at high oxygen pressures, the ionic conductivity is comparable to that of Y_2O_3-stabilized ZrO_2 (with 8% Y_2O_3), the model solid electrolyte.[22] Therefore, $Sr(Ti,Fe)O_3$ solid

solutions make interesting SOFC cathode materials. On the other hand, substituting La for Sr or Nb for Ti makes $SrTiO_3$ an *n*-type conductor whose electronic conductivity extends over many orders of magnitude (depending upon the conditions), exhibiting metallic or semiconducting behavior at intermediate and high temepratures.[9,12,23,24] Thin films of *n*-doped ($Sr_{1-x}La_xTiO_3$) and *p*-doped ($SrTi_{1-y}Fe_yO_3$) therefore serve as the model electrode materials in this study. In year one, the focus was placed on *p*-doped ($SrTi_{1-y}Fe_yO_3$).

Phase I objectives included the preparation of characteristic compositions within the STF system and the characterization of their microstructure and chemical composition. First targets for pulsed laser deposition (PLD) with x = 0.05 (STF05) and 0.35 (STF35) were prepared. Thin films (thickness between 60 and 200 nm) of STF35 were deposited by PLD on Al_2O_3 (sapphire) and MgO substrates ($10\times10\times0.5$ mm^3, 2-side polished, MTI Crystals, Richmond, CA). The films were shown via XRD and AFM to be polycrystalline (grain size $\leq$100nm) and of the expected perovskite structure with some degree of preferential orientation along the (110) direction was observed (see Fig.5). The chemical composition of the films was examined using Rutherford Backscattering Spectrometry (RBS) and was found to be commensurate with the composition of the target material. Electrical characterization (not reported here) were largely consistent with our earlier studies of bulk STF ceramics[25]. In addition to PLD samples, STF films (x=0.1, 0.35) were deposited onto single crystal YSZ (100) or (111) substrates by thermal ink-jet (TIJ) printing, given its convenience for depositing and screening ternary or quaternary ceramic compounds and the need for only small amounts (~ 1 ml) of precursor solution[26]. Following firing at 1100 °C for 3h in air, XRD patterns confirmed, as well, the formation of the perovskite phase.

In addition to conventional gas sensor tests, the TIJ (thermal ink jet) deposited $SrTi_{1-x}Fe_xO_{3-\delta}$ films were used as model materials for fuel cell electrodes. The layers were deposited on single crystal YSZ (100) or (111) substrates using the MIX precursor approach. The TIJ ink contained stoichiometric amounts of strontium nitrate, titanium iso-propoxide, and iron nitrate in aqueous

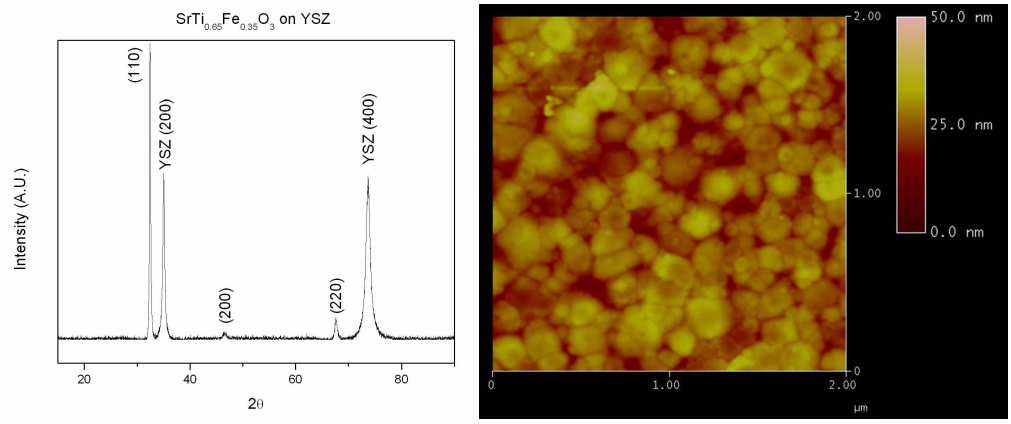

Figure 5: XRD and AFM of STF35 films deposited onto YSZ

solution, the pH was adjusted using glacial acetic acid. In a first series, two STF compositions were prepared with x = 0.10 and x = 0.35. The nozzle size was C-220. Prior to deposition, the substrates were ultra-sonicated in DI water and iso-propanol and rinsed with acetone. After deposition, the films were fired at 1100 °C for 3h in air.

The XRD patterns on the TIJ films (Fig. 6) showed perovskite peaks plus some minor impurity peaks. Since the latter were also present after film removal and could not be attributed to any other Sr, Ti or Fe phase, the TIJ films were assumed to be highly pure perovskite.

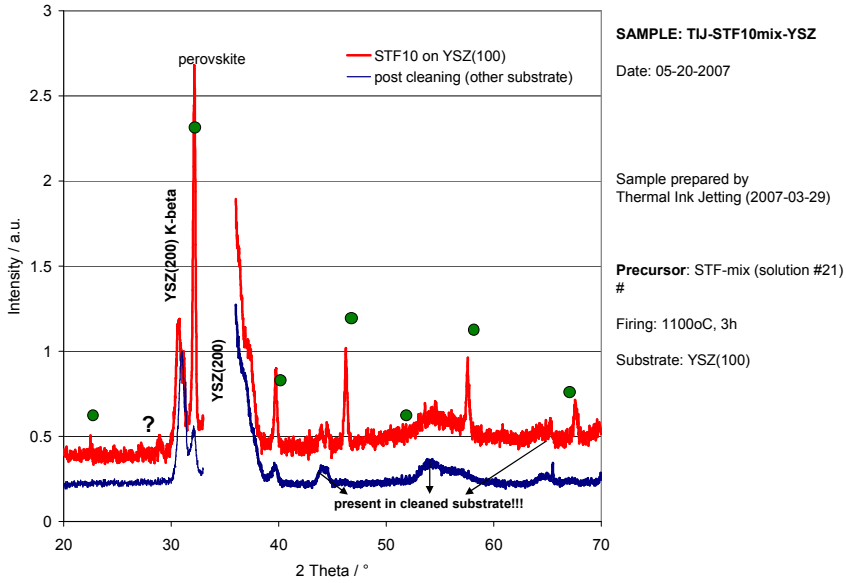

Figure 6: XRD on TIJ deposited STF10 film on YSZ single crystal substrate.

For one set of electrochemical cell measurements, Fig. 7, either Pt ink or Ag paste was painted on the backside of the YSZ samples. For a second test series, Fig. 8, symmetrical STF electrodes were prepared on YSZ(111) with x = 0.05, x = 0.35, and x = 0.50 with an area of 7 mm². Again, the nozzle size was C-220, and the substrates were ultra-sonicated in DI water and iso-propanol and rinsed with acetone. After deposition, the films were fired at 1100 °C for 3h in air.

These samples were measured in a tube furnace in the temperature range from 500 °C to 900 °C with different pO_2. To provide current collector contacts, the symmetrical samples were sandwiched between Au mesh pressed down with Pt wires. Impedance spectra were collected with a Solartron 1260 analyzer.

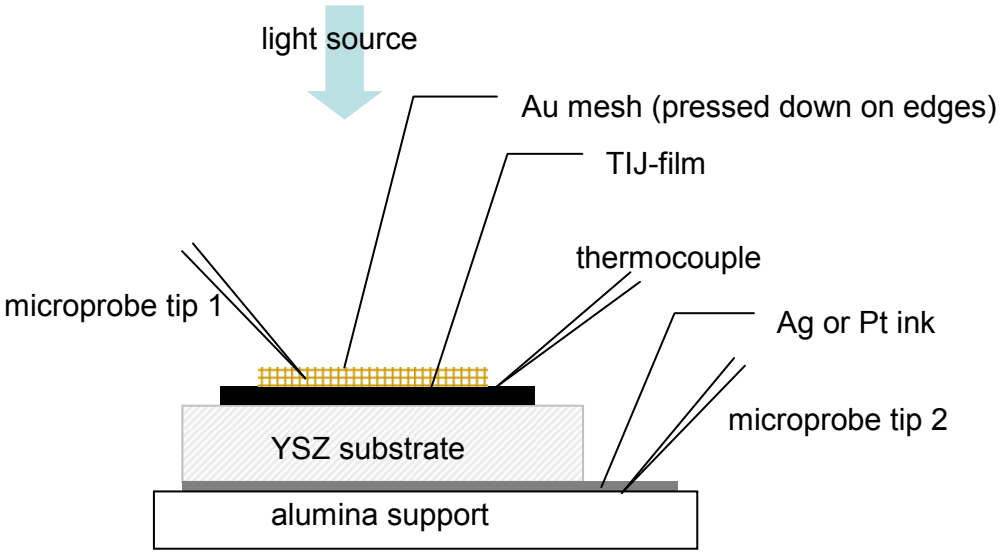

Figure 7: set-up for microprobe measurements.

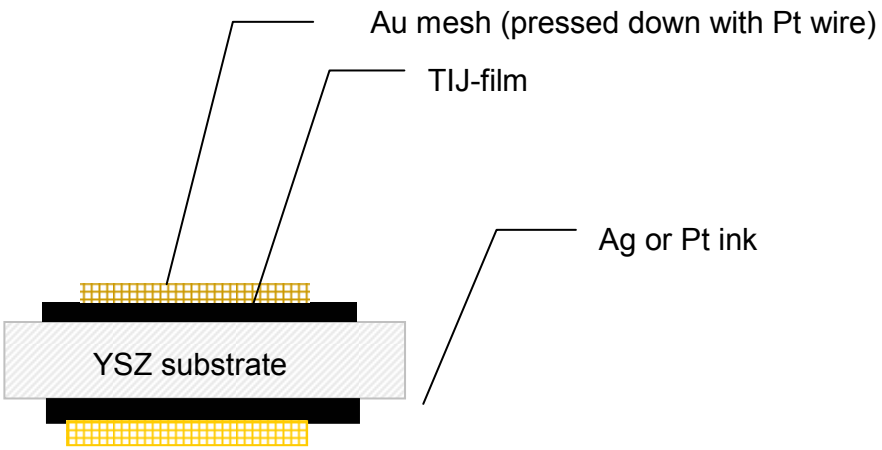

Figure 8: Symmetrical sample on YSZ single crystal

C. Characterization Approach: Kelvin Probe, Illumination & Impedance

Measurement techniques were selected which provide the ability to isolate the contributions of e.g. gas adsorption, charge transfer and diffusive kinetics towards the overall electrode impedance. Towards this end, a unique microprobe system was designed and assembled which allows for the characterization of thin films with microelectrodes under elevated temperatures and controlled atmospheres. The system was outfitted during Phase I with a built-in Kelvin Probe (Fig. 9) and offers the option for broad band and monochromatic illumination in conjunction with Kelvin Probe and complex impedance measurements.

These techniques are being used interactively, in novel ways, to achieve new insights into the relative importance of these electrode processes.

Illumination and Impedance Spectroscopy: In this research project, we proposed a novel approach to enable reduction in operating temperature by the use of illumination to promote cathodic and anodic reactions at reduced temperatures. At a minimum, this will serve as a powerful tool in investigating charge transfer reactions at SOFC electrodes. Potentially, it will serve to *photo-catalyze* the electrode reactions and enable lower temperature operation with improved conversion efficiency.

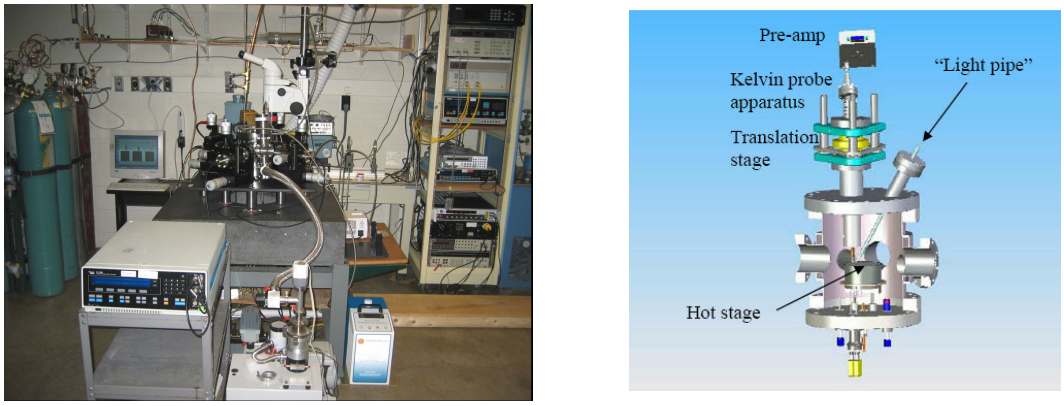

Figure 9: Photograph of the Microprobe Characterization System and Kelvin Probe attachment.

The effect of light, primarily in the UV range, in promoting redox processes on wide-bandgap metal-oxide catalysts is well known in the photocatalysis literature.[27,28] This effect has been utilized in various electrochemical systems such as photo-anodes for water photolysis,[29] dye-sensitized solar cells,[30] and photocatalysts for oxidation of deleterious organic molecules for waste treatment.[31] This approach has been applied largely to solid/liquid interfaces at ambient temperatures (~25°C), while little is known about solid/gas systems at elevated temperatures.

Recent reports on the effect of UV light in enhancing the rate of oxygen incorporation into Fe-doped $SrTiO_3$, a model *p*-type mixed conductor, at temperatures between 540 and 730°C,[32,33] suggest that this effect can be harnessed to improve the electrochemical performance of SOFC cathodes, particularly at low operation temperatures (< 600°C). A reduction in the activation energy from 274 kJ/mole in dark to 145 kJ/mole in UV light conditions has been reported, leading to more than a *hundredfold* increase in the rate of oxygen incorporation at 540°C.[32] This dramatic effect has been attributed to photo-generation of electrons followed by their transfer to oxygen adsorbates at the surface of $SrTiO_3$.[33] Similarly to Fe-doped $SrTiO_3$, SOFC cathodes such as LSM and LSC and our model STF system are also *p*-type conductors where the availability of conduction band electrons to be transferred to oxygen adsorbates is scarce at low temperatures. Therefore, photo-generation of these carriers by absorption of UV light is expected to enhance the cathodic reaction, particularly at low temperatures.

Impedance studies of STF electrodes on YSZ in Phase I resulted in typical spectra expected for cathodes and so demonstrate the utility of our selection of the STF model system. The spectra (see Fig. 10) fit very well to equivalent circuit models. These elements have been examined as functions of temperature and pO_2 and corresponding activation energies and pO_2 dependencies derived. At low temperatures, a Warburg signature spectrum is obtained pointing to a diffusion controlled process. These parameters are now being studies as functions of STF composition, bias and illumination and in concert with work function studies. Preliminary results confirm that the impedance decreases with increasing area rather than increasing perimeter of the electrode, consistent with the MIEC nature of STF.

Preliminary studies examining the effect of illumination have been encouraging. Figure 11 compares the impedance response in the dark and under broadband illumination of the light source. We estimate that the effective illumination power contained in the UV range (~200-400 nm) of interest is equal to ~30-60 mW or less. Yet, the electrode impedance was reduced by 73% reduced under illumination.

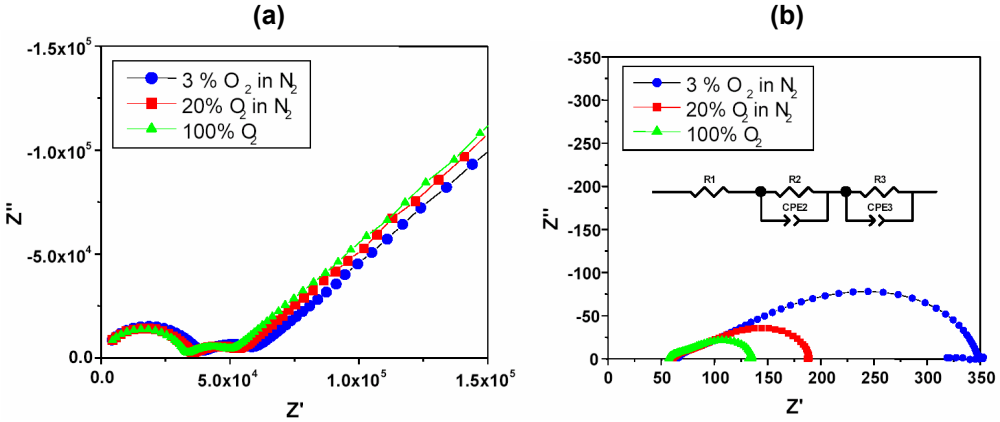

Figure 10: Impedance spectra of symmetrical STF35-YSZ cells a) at 400°C; b) 900 °C. Oxygen partial pressure as indicated. Inset: Equivalent circuit used for data fitting.

Kelvin Probe: Various techniques are used to examine surface or near surface properties of SOFC electrodes including X-ray photoelectron spectroscopy (XPS), Auger electron spectroscopy (AES) and secondary ion mass spectroscopy (SIMS). However, they are not in-situ methods and are generally limited to RT and high vacuum conditions. Complex impedance spectroscopy can be examined in-situ, but there are contributions from non-surface related processes (e.g. bulk diffusion) and it is poor in its ability to monitor rapid kinetics given that electrode processes fall at low frequencies. The *Kelvin Probe (KP)*, on the other hand is non-invasive, yet is extremely sensitive to changes in the top-most atomic layer as reflected in measured changes in the *work function (WF)* of the material being studied. This technique is of interest in this program given that the work function is directly implicated in surface processes such as chemisorption and oxygen incorporation into the electrode. The instrument installed in our microprobe system is based on the McAllister KP-6500 Kelvin probe, but the design was modified by us in collaboration with McAllister personnel to allow for a) high- temperature

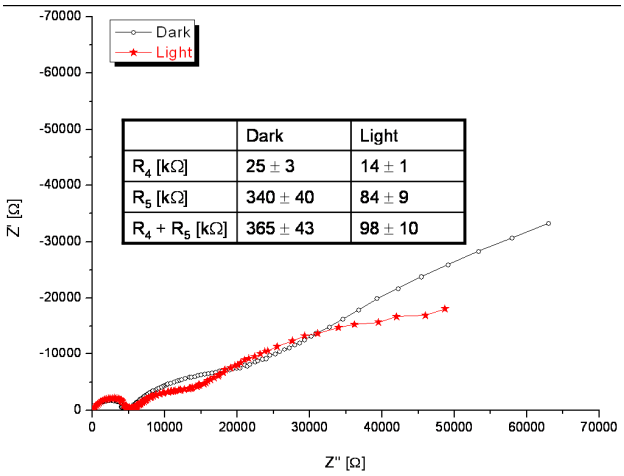

	Dark	Light
R_4 [kΩ]	25 ± 3	14 ± 1
R_5 [kΩ]	340 ± 40	84 ± 9
$R_4 + R_5$ [kΩ]	365 ± 43	98 ± 10

Figure 11: Impedance spectra with STF35 electrode, at T = 400°C, in air (flow rate = 400sccm), under anodic polarization of 100 mV. The response under dark is shown in black, the response in low-power broadband light conditions shown in red. The inset table shows the respective electrode resistances R4 and R5.

measurements (up to ca. 800°C) by incorporating water-cooling around the temperature-sensitive oscillation apparatus, and b) for surface photovoltage spectroscopy (SPS) measurements by incorporating a light-guide. Therefore, the *KP* can be an effective tool for studying the surface properties under high temperature and gas controlled environments. The significance for our research is now reviewed.

Surface charge transfer interactions such as *chemisorption* result in surface depletion or double layer formation with resultant *WF* changes. By proper analysis, it becomes possible to identify the *surface chemisorbed species and their degree of surface coverage,* very important for understanding the rate limiting step of SOFC electrode reactions and ultimately reducing electrode polarization losses. Since the *WF* reflects the Fermi-level position, changes induced in the Fermi level by *changes in stoichiometry* can also be detected. Because the work function is only sensitive to the outermost surface, one can distinguish changes in *defect chemistry* of the top surface out of that of the bulk material. By examining the time dependent change in WF in a SOFC electrode upon a change in pO_2, temperature or bias, it becomes possible to discriminate between the rapid chemisorption and the slower stoichiometry change kinetics[34]. We have initiated such studies both on LSC30 and STF35 and we indeed see the signatures of the respective kinetics as illustrated in Fig. 12. The changes in Contact Potential Difference

(CPD), the difference in WF between the specimen and the reference electrode, in response to changes in pO_2 were large, rapid and reversible. Both LSC and STF electrodes showed similar behavior.

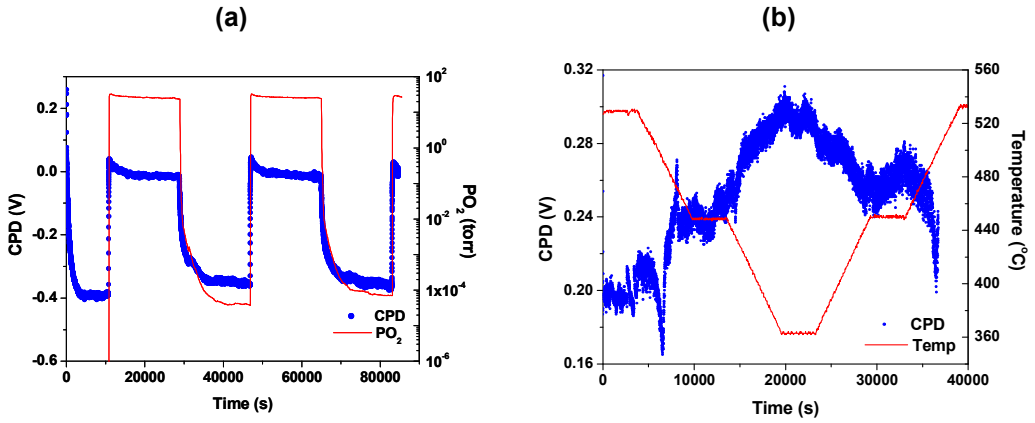

Figure 12: CPD changes measured on $La_{0.7}Sr_{0.3}CoO_3$: a) under the periodic pO_2 change at 530°C; b) as a function of temperature with 100% O_2 gas flowing.

In case of LSC ~400mV changes in CPD were induced initial rapid increase is consistent with chemisorption of negatively charged oxygen species on the LSC and STF electrodes. At longer times, oxygen incorporation into the electrodes leads to decreases in Fermi level, which in turn enhances oxygen desorption resulting in a decrease in WF as reported by Nowotny, et. al.[34] In this way, they derived the chemical diffusion coefficient associated with stoichiometry changes by four orders of magnitude change in pO_2. As seen in Fig 12a, the WF increases rapidly upon increase in pO_2 followed by a much slower decrease. By reducing the temperature to where oxygen exchange between the gas phase and the bulk becomes very sluggish, it becomes possible to focus only on chemisorption effects. Likewise, at very elevated temperatures, where chemisorption effects are small, stoichiometry change kinetics can be readily resolved. Fig. 12b, shows both the reversible response of the CPD to temperature and the ability to resolve changes on the order of 10 mV. Fig. 13 shows CPD data for STF 35 under similar periodic pO_2 changes but at lower temperature (410°C). Here the CPD changed by ~200mV, about half that observed for LSC, suggesting a smaller change in chemisorbed oxygen. Further, as expected, increasing temperature leads to increasing oxygen desorption and thereby decreasing *WF*.

These data also show that we were able to examine the influence of broad band illumination while performing the CPD measurements under controlled temperature and pO_2. No significant changes could be detected here. We are presently beginning to investigate how much light actually reaches the electrode region under the Kelvin probe by replacing the specimen with a photodiode and will be installing the ability to modulate the light intensity in concert with a lock-in-amplifier to enable higher resolution of light induced effects.

While the *KP* has been applied towards examining the surface exchange reaction, very limited studies have been performed under electrical and electrochemical driving forces relevant to SOFC operating conditions. It is well known that the catalytic activity of metals can be altered dramatically and reversibly by supplying or removing oxide anions, O^{2-}, at the metal catalyst surface, by interfacing with an electrolyte such as zirconia. This effect is termed the non-faradaic electrochemical modification of catalytic activity (NEMCA).[35] By Kelvin probe measurements, it is possible to monitor the formation of the electrochemically driven oxygen double layers and even identify the ionization number of the surface adsorbed oxygen species. Also, since the oxidation catalytic activity is very sensitive to the work function change of the

electrode materials, the *KP* technique provides the relation between catalytic activity in the SOFC anode and the electrochemical polarization. The phase stability of materials, as well as segregation, can be detected by *KP* measurements given their surface sensitivity. This will be used to our benefit to detect and correlate the formation of reaction products or segregants with changes in electrode performance.

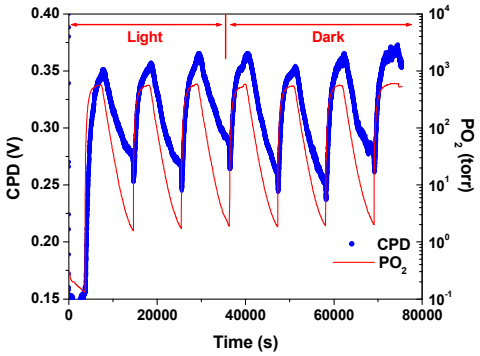

Figure 13: CPD of $SrTi_{0.65}Fe_{0.35}O_3$ as function of time at 410°C under periodic pO_2 changes both in the dark and under illumination.

Recent studies with metal oxide sensors suggests that UV light may be beneficial in promoting oxidation of reducing gases on their surfaces, resembling the anodic reaction in SOFC.[36,37,38]. We expect that UV light could promote the anodic reaction process by providing photo-generated holes to break the chemical bonds with surface oxide ions or intermediate complexes between oxide ions and fuel adsorbates (e.g., OH^-). We also expect that narrow bandwidth light could promote desired redox processes selectively by tuning the wavelength to excite the respective states. Light-based spectroscopic techniques such as Surface Photovoltage Spectroscopy (SPS) provide a powerful tool to investigate surface states on surfaces by monitoring changes in *WF* due to photo-excitations of these states[39]. We propose to extend this principle to manipulate selectively redox processes that involve different electronic states. This approach may become particularly important in single-chamber fuel cells that operate in a gas mixture comprising both the fuel and oxygen mixed together in the same compartment[40]. Hence, their performance largely depends on the capability of the electrodes to selectivity favor the oxygen reduction reaction on the cathode and fuel oxidation on the anode[41].

3. Conclusion:

This program has several inter-related objectives. Most broadly, to identify electrodes that will make it possible to significantly reduce the operating temperature of micro-SOFC and thin film-based SOFCs. Towards that objective, 1) identify the key rate limiting steps limiting presently utilized electrodes from performing at reduced temperatures and 2) investigate the use of optical as opposed to thermal energy as a means for photocatalyzing electrode reactions and enabling reduced operating temperatures. As we discussed above, this requires a multifaceted approach which addresses the need to a) work with well defined and reproducible electrode structures and model electrode compositions thereby enabling conclusions to be made about the rate limiting mechanisms controlling electrode performance which can then be broadly applied, b) utilize measurement techniques, including illumination, Kelvin Probe and Impedance Spectroscopy, which provide the ability to isolate the contributions of e.g. gas adsorption, charge transfer and diffusive kinetics towards the overall electrode impedance and c) offer

prototype structures demonstrating reduced temperature operation and the potential advantages of illumination.

In phase I, we have focused on a) assembling and testing our unique Microprobe Thin Film Characterization System, b) demonstrating that the model materials system can be fabricated in thin film form, c) that it exhibits expected physical properties and d) that it can be configured and operated as model cathode materials. A key objective was also to test the potential of illumination in enhancing electrode performance. These were all achieved.

III. LIST OF ACRONYMS AND ABBREVIATIONS

CPD	Contact potential difference.
IS	Impedance spectroscopy
KP	Kelvin Probe
MIEC	Mixed Ionic-Electronic Conductor
PLD	Pulsed Laser Deposition
SOFC	Solid Oxide Fuel Cell
SPS	Surface Photovoltage Spectroscopy
STF	$SrTi_{1-y}Fe_yO_3$
WF	Work Function
YSZ	$Y_yZr_{1-y}O_{2-y/2}$

IV. REFERENCES/BIBLIOGRAPHY

[1] A. Bieberle-Hütter, M. Søgaard and H. L. **Tuller**, "Electrical and Electrochemical Characterization of Microstructured Thin Film $La_{1-x}Sr_xCoO_3$ Electrodes", Solid State Ionics, **177**, 1969-1975 (2006).

[2] J. Hertz, Microfabrication Methods to Improve the Kinetics of the Yttria Stabilized Zirconia – Platinum – Oxygen Electrode, PhD thesis, MIT, Sept. 2006.

[3] J. Hertz and H.L. **Tuller**, "Nanocomposite Platinum-Yttria Stabilized Zirconia Electrode and Implications for Micro Solid Oxide Fuel Cell Operation", J. Electrochem. Soc., accepted for publication (1/4/07).

[4] J. Fleig, F.S. Baumann, V. Brichzin, H.R. Kim, J. Jamnik, G. Cristiani, H.U. Habermeier, and J. Maier, "Thin film microelectrodes in SOFC electrode research", *Fuel Cells*, ***3-4*** (2006), 284-292.

[5] H. Huang, M. Nakamura, P. Su, R. Fasching,Y. Saito, and F B. Prinz, High-Performance Ultrathin Solid Oxide Fuel Cells for Low-Temperature Operation, *Journal of The Electrochemical Society,* 154 (2007) B20

[6] K. van Benthem, C. Elsässer, and R. H. French, J. Appl. Phys. 90 (2001) 6156.

[7] C. Lee, J. Destry, and J. L. Brebner, Phys. Rev. B 11 (1975) 2299.

[8] D. Goldschmidt and **H. L. Tuller**, Phys. Rev. B 35 (1987) 4360.

[9] N.-H. Chan, R. K. Sharma, and D. M. Smyth, J. Electrochem. Soc. 128 (1981) 1762.

[10] G. M. Choi and **H. L. Tuller**, J. Am. Ceram. Soc. 71 (1988) 201.

[11] I. Denk, W. Münch, and J. Maier, J. Am. Ceram. Soc, 78 (1995) 3265.

[12] R. Moos and K. H. Härdtl, J. Am. Ceram. Soc. 80 (1997) 2549.

[13] G. M. Choi, **H. L. Tuller**, and D. Goldschmidt, Phys. Rev. B 34 (1986) 6972.

[14] M. Fleischer, H. Meixner, and C. Tragut, J. Am. Ceram. Soc. 75 (1992) 1666.

[15] R. Moos, W. Menesklou, and K. H. Härdtl, Appl. Phys. A 61 (1995) 389.

[16] J. Claus, M. Leonhardt, and J. Maier, J. Phys. Chem. Solids 61 (200) 1199.
[17] Y. Adachi, S. Kohiki, K. Wagatsuma, and M. Oku, J. Appl. Phys. 84 (1998) 2123.
[18] G. Borstel, R. I. Eglitis, E. A. Kotomin, and E. Heifets, phys. stat. sol. (b) 236 (2003) 253.
[19] I. Denk, J. Claus, and J. Maier, J. Electrochem. Soc. 144 (1997) 3526.
[20] R. Waser and R. Hagenbeck, Acta. Mater. 48 (2000) 797.
[21] F.D. Gealy and **H.L. Tuller**, in Proc. Symp. Electro-Ceramics and Solid State Ionics, eds. H.L. Tuller and D.M. Smyth, The Electrochemical Society, Pennington, NJ, 1988, pp. 23-34.
[22] V. V. Kharton, A. V. Kovalevsky, A. P. Viskup, J. R. Jurado, F. M. Figueiredo, E. N. Naumovich, and J. R. Frade, J. Solid State Chem. 156 (2001) 437.
[23] T. Inoue, N. Seki, J. J. Kamimae, K. Eguchi, and H. Arai, Solid State Ionics 48 (1991) 283.
[24] J. C. C. Abrantes, J. A. Labrincha, and J. R. Frade, Sens. Actuators B 56 (1999) 198.
[25] A. Rothschild, W. Menesklou, H. L. **Tuller** and E. Ivers-Tiffée, "Electronic Structure, Defect Chemistry, and Transport Properties of $SrTi_{1-x}Fe_xO_{3-y}$ Solid Solutions", *Chem. Mater.* ***18,*** 3651-3659 (2006).
[26] Wang, J., Mohebi, M., Evans, J., Two methods to generate multiple compositions in combinatorial ink-jet printing of ceramics, Macromol. Rapid Commun. 26 (2005), 304-309
[27] T. Wolkenstein, *Electronic Processes on Semiconductor Surfaces during Chemisorption* (Consultants Bureau, New York, 1991).
[28] R. Memming, *Semiconductor Electrochemistry* (Wiley-VCH, Weinheim, 2001).
[29] A. Fujishima and K. Honda, *Nature* 238 (1972) 37.
[30] B. O'Regan and M. Grätzel, *Nature* 353 (1991) 737.
[31] M. R. Hoffmann *et al*., *Chem. Rev.* 95 (1995) 69.
[32] R. Merkle, R. A. De Souza, and J. Maier, *Angew. Chem. Int. Ed.* 40 (2001) 2126.
[33] R. Merkle and J. Maier, *Phys. Chem. Chem. Phys.* 4 (2002) 4140.
[34] J. Nowotny, T. Bak, and C.C. Sorrell, "Charge transfer at oxygen/zirconia interface at elevated temperatures - Part 8", *Advances in Applied Ceramics*, ***104*** (2005), 200-205.
[35] C.G. Vayenas, S. Bebelis, and S. Ladas, "Dependence of Catalytic Rates on Catalyst Work Function," *Nature*, 343 (1990), 625
[36] E. Comini *et al*. Sens. Actuators B 65 (2000) 260; *ibid.* 78 (2001) 73.
[37] K. Anothainart *et al.* Sens. Actuators B 93 (2003) 580.
[38] E. Comini *et al.*, *IEEE Sensors J.* 4 (2004) 17.
[39] L. Kronik and Y. Shapira, *Surf. Sci. Rep*. 37 (1999) 1.
[40] T. Hibino et al., *Science* 288 (2000) 2031.
[41] I. Riess, P. J. van der Put, and J. Schoonman, *Solid State Ionics* 82 (1995) 1.